ELSEVIER

International Journal of Mass Spectrometry 185/186/187 (1999) 401–412

International Journal of Mass Spectrometry

Chiral recognition and the deprotonation reaction of gas-phase cytochrome *c* ions

Shuinu Gong, Elvira Camara, Fei He, M. Kirk Green, Carlito B. Lebrilla*

Department of Chemistry, University of California, Davis, CA 95616, USA

Received 5 June 1998; accepted 9 August 1998

Abstract

Gas-phase deprotonation reactions of cytochrome *c* ions by chiral amines (2-butylamine and 1-amino-2-propanol) exhibit strong chiral specificity. The *R*-isomer of 2-butylamine is at most 10 times more reactive than the *S*-isomer. With 1-amino-2-propanol, the *R*-isomer is as much as two times more reactive than the *S* isomer. The specificity decreases with increasing charge states. For the 12+ state, the (2*R*)-2-butylamine is only 50% more reactive than the *S* isomer, compared to 10 times for the 9+ state. Reactions of the racemic mixture of 1-amino-2-propanol and double resonance experiments suggest a complicated proton transfer mechanism possibly involving a diadducted intermediate—the protein with two alkyl amine adducts. Variable temperature experiments are also performed to illustrate the presence of a barrier in the proton transfer reaction. (Int J Mass Spectrom 185/186/187 (1999) 401–412) © 1999 Elsevier Science B.V.

Keywords: Chiral recognition; Deprotonation reaction; Gas phase

1. Introduction

As the complexity of the compounds studied with mass spectrometry increases, information beyond molecular weight and connectivity is required. The stereochemistry of compounds are not traditionally obtained from mass spectrometry; however, the use of mass spectrometry either in conjunction with a separations method or directly to probe the stereochemistry has received increasing attention [1–25]. Previous studies have concentrated primarily on differentiating stereochemistry based on ionization efficiencies. The energy acquired by the ion during ionization produces metastable dissociation reactions whose rates vary depending on the stereochemistry of the analytes. Fourier transform ion cyclotron resonance (FTICR) spectroscopy traps ions for long periods making it highly amenable for exploring the effect of chirality on ion/molecule reactions. Nonetheless, there are only a few examples of chiral recognition in gas-phase ion/molecule reactions. Chu et al. have observed chiral selectivity in the complexation of a host molecule containing two stereocenters with a chiral guest [26]. Nikolaev et al. have shown chiral effects in the unimolecular dissociation and ligand exchange of proton bound dimers of dimethyl tartrates [27,28].

Ion/molecule reactions involving enantiomerically pure compounds can be developed to probe multiply protonated proteins. The nature of the protein surface as well as the steric and electrostatic environment of

* Corresponding author.

Dedicated to Professor Michael T. Bowers on the occasion of his 60th birthday.

1387-3806/99/$20.00 © 1999 Elsevier Science B.V. All rights reserved
PII S1387-3806(98)14148-9

the sites of protonation may be explored. In a previous article, we reported that the gas-phase proton transfer reactions of (2*R*)- and (2*S*)-2-butylamine with three charge states of cytochrome *c* (9+, 8+, and 7+) exhibit marked chiral specificity [29]. In these systems, the reactants, the multiprotonated cytochrome *c* $[MH_n]^{n+}$ and base B, react to produce at least three major ionic products: an adduct of the base $[MBH_n]^{n+}$, a deprotonated product $[MH_{(n-1)}]^{(n-1)+}$, and a base adduct of the deprotonated product $[MBH_{(n-1)}]^{(n-1)+}$. A strong systematic preference for the *R*-enantiomer over the *S* was observed. The rate constants of reactions involving the *R* enantiomer are about 10 times greater than those involving the *S*. For comparison, *n*-propylamine and *t*-butylamine were reacted with the same three charge states of cytochrome *c*. *n*-Propylamine in many instances reacted with similar rate constants to *S*-2-butylamine, while *t*-butyl amine was the least reactive of the four amines despite its having the largest gas-phase basicity.

In this work, we explore further the effect of higher charge states and more basic chiral reagents on the deprotonation reaction of cytochrome *c*. The mechanism of proton transfer involving amines and gas-phase proteins is probed to better understand the nature of chiral specificity.

2. Experimental

The multiply charged ions were produced by electrospray ionization (ESI) [30–32]. Proton transfer reactions were monitored in a home-built Fourier transform mass spectrometry (FTMS) instrument. The instrument contains a dual chamber with rapidly interchangeable fast atom bombardment ionization, matrix-assisted laser desorption/ionization (MALDI), and ESI sources. Proton transfer reactions are performed using procedures described in greater detail elsewhere [33–35]. Briefly, ions produced by ESI are guided through a single stage quadrupole ion guide into a cubic analyzer cell. The detection electrodes of the analyzer cell are connected to a set of internal preamplifiers. Ions injected from the source are translationally cooled using a nitrogen pulsed gas that produces a maximum pressure of 10^{-5} Torr. The base pressure is obtained 3 s after the pulse. The operations of the instrument are controlled by an Omega Data system (IonSpec). The five stages of differential pumping maintain a pressure of 10^{-10} Torr in the analyzer region during normal operation. Proton transfer reactions are performed by first purifying the amine with at least three freeze–thaw cycles before introducing it into the analyzer cell with a precision leak valve. For consistency, a pressure of approximately 1×10^{-7} Torr is maintained for all the experiments. The pressure is corrected using published calibration methods [36].

Deprotonation reactions at elevated temperatures were performed with the chamber heated by a large silicon heater that spanned the full length of the analyzer chamber. Temperatures were monitored in the analyzer cell and the chamber wall with a type *K* thermocouple during the experiment. Experiments were performed when the chamber wall was in thermal equilibrium with the thermocouple placed in the center of an auxiliary analyzer cell adjacent to the main analyzer cell. The reagent gases were leaked into a heated tube (100 °C) before introduction into the main chamber.

Samples were prepared either by directly dissolving cytochrome *c* in a 50:50 H_2O/CH_3OH solution or in a 1:49.5:49.5 acetic acid/H_2O/CH_3OH solution. Horse heart cytochrome *c* was obtained from Sigma (St. Louis, MO) and used without further purifications. (2*S*)- and (2*R*)-2-butylamine, and (2*S*)- and (2*R*)-1-amino-2-propanol were obtained from Aldrich (Milwaukee, WI) in purities greater than 99% and were used without further purifications.

3. Results

3.1. Reactions of (2R)- and (2S)-2-butylamine with 7+ to 12+ charge states of cytochrome c

Fig. 1 shows a series of spectra beginning with the isolated 8+ charge state (8 in bottom trace) in the presence of 1.0×10^{-7} Torr (2*R*)-2-butylamine. Adducts consisting of cytochrome *c* and one amine

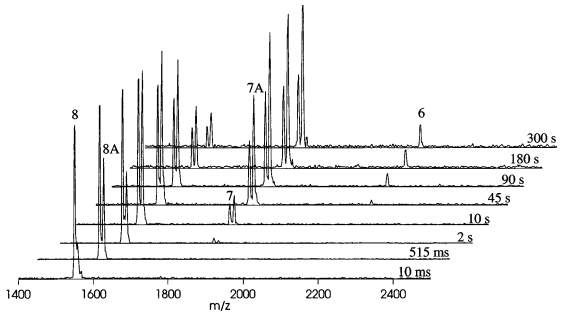

Fig. 1. The spectra of an isolated 8+ charge state of cytochrome *c* in the presence of 1×10^{-7} Torr (2*R*)-2-butylamine. The monoadducted species is designated by *A*.

molecule (8*A*) formed within 100 ms after the ion forming and trapping events. The intensities of the adducted species continue to grow with time to become as large as that of the uncomplexed cytochrome *c* ions. The intensity of the deprotonated product, the 7+ state, is observable after approximately 2 s (7 and 7*A*). The doubly deprotonated product, the 6+ state, is observed after approximately 40 s.

Experiments were performed to determine the rate constants for the formation of the adduct of 2-butylamine and the 8+ charge state of the protein. Ejection of the adduct was performed to isolate the uncomplexed ionic species. However, adduct formation occurred rapidly at rates corresponding approximately to collision rates. Selective ejection of the uncomplexed 8+ species isolated the monoadduct. The uncomplexed 8+ species also formed readily and was observed 100 ms after the isolation event. Because the ions are no longer transported from the source at this point in the experiment, the uncomplexed species can only come from the dissociation of the complex. These experiments provided indications

$$[MH_n]^{n+} + B \underset{k_r = \text{Fast}}{\overset{k_f = \text{Fast}}{\rightleftharpoons}} [MBH_n]^{n+}$$

Scheme 1

that the adduct ions $[MBH_n]^{n+}$ (Scheme 1) and the cytochrome *c* ions $[MH_n]^{n+}$ are in rapid equilibrium during the experiment. The rates and rate constants for adduct formation were obtained from these exper-

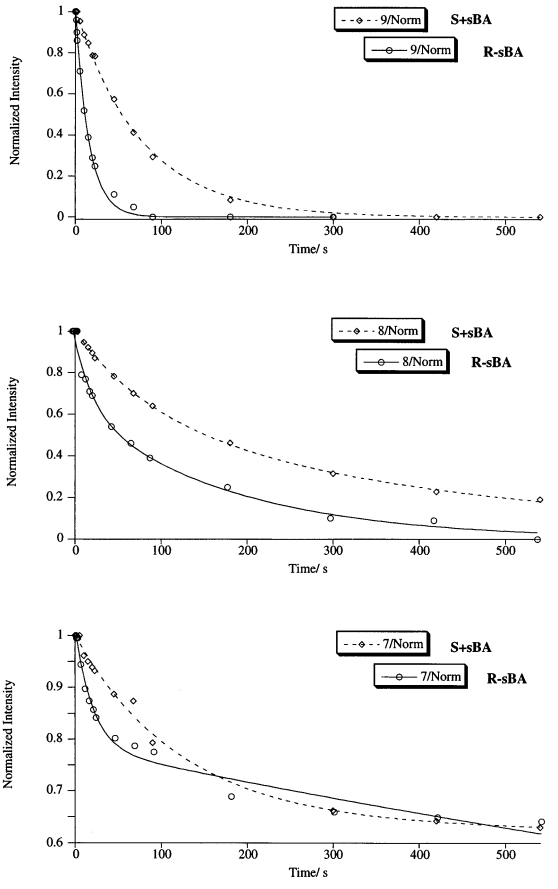

Fig. 2. The dependence of intensity on time measured by FTMS of selected charge states of cytochrome *c* reacting with 1×10^{-7} Torr of 2-butylamine.

iments, but the results varied widely between experiments. We believe that the isolation of the adduct by selective ejection also translationally excited the uncomplexed ionic species leading to irreproducible rates.

The procedure for determining reaction rates and rate constant involves monitoring the reactant ion and the product ion as a function of time. The relative intensities of the 9+ and 8+ state in the presence of (2*R*)- and (2*S*)-2-butylamine (1×10^{-7} Torr) as a function of time is shown in Fig. 2. From these plots, the greater reactivity of the *R*-isomer is readily apparent. Rate constants were obtained by considering several equilibrium reactions and solving a set of coupled differential equations using a procedure de-

Table 1
Rate constants[a] of deprotonation reactions involving amines and various charge states of cytochrome *c* ions from solutions of 50:50 H_2O:MeOH with 1% HAc. The mass selected ion is the highest charge state in the group

Charge states[b]	(*R*)-(−)-*s*-$BuNH_2$	(*S*)-(+)-*s*-$BuNH_2$
12+ to 11+	310	220
11+ to 10+	130	4.4
10+ to 9+	37	3.2
9+ to 8+	16	0.91
11+ to 10+	160	140/4.3 (52:48)[c]
10+ to 9+	63	3.0
9+ to 8+	18	1.5
10+ to 9+	70	5.1
9+ to 8+	23	1.6
8+ to 7+	6.1	0.62
9+ to 8+	18	1.8
8+ to 7+	2.8	0.33
8+ to 7+	13/1.6 (45:55)[c]	0.53
7+ to 6+	11/0.13 (41:59)[c]	0.038

[a] $\times 10^{-12}$ of cm^3/molecule s.
[b] The higher charge state in each group is isolated from the ion source. All others are formed by deprotonation reactions.
[c] Percent contribution from the fast and slow reacting species.

scribed in earlier publications [37–39]. The intensities of the charge state and its adduct were summed in the analyses.

The rate constants obtained from the proton transfer reactions of the two isomers of 2-butylamine with the 7+ to 12+ charge states of cytochrome *c* are listed (Table 1). The standard deviations calculated from the statistical analysis of the fitting function are typically less than 20%. The determination of precise values are complicated by the determination of the pressure [34,35]. We use a gas-phase ion/molecule reaction to calibrate the ion gauge [36]. This method allows reliable determination of the pressure to only a factor of 2 or 3. However, because enantiomers have nearly identical physical properties, the relative rate constants of the enantiomers should not be affected by differences in ion gauge sensitivities. Direct comparisons of rate constants of enantiomers can be performed much more reliably than the direct comparisons of rate constants from different (nonenantiomeric) amines.

The rate constants vary from low 10^{-13} to 10^{-10} (cm^3/molecule s) for 2-butylamine. Cytochrome *c* ions produced from a mixture of 1% acetic acid in a 49.5:49.5 ratio of H_2O/CH_3OH and those produced from 50:50 H_2O/CH_3OH, published earlier [29], have similar rate constants. The rate constants of cytochrome *c* produced with the two different preparations are essentially the same for the 7+, 8+, and 9+ charge states reacting with the *R* isomer. For the *S*-isomer, the fast reacting components are not observed with the 7+ and 8+ states. Acidifying the solvent does not appear to strongly affect the reactivity of cytochrome *c*, as previously reported [38]. In that work, it was suggested that the ESI conditions denature cytochrome *c*, while acidifying the solution does not further denature the protein. Similar conclusions are reached with the enantiomers of 1-amino-2-propanol, as we will show in the following.

With every charge state, the *R*-isomer of 2-butylamine is more reactive than the *S*. With the charge states 8+, 9+, 10+, and 11+, the *R*-isomer is approximately 10 times more reactive than the *S*. The 11+ species exhibits reactivity consistent with at least two populations that have different rates of reaction with the *S* isomer. The slow reaction has a rate constant that is an order of magnitude lower, while the fast reaction has a rate constant that is nearly equal to the *R* isomer. For the 12+ charge state, both *R* and *S* are of equal magnitude, with the rate constant for the *R* only about 50% greater than that for the *S*.

The increase in the rate constants and the decrease in the chiral specificity is consistent with the increase in Coulombic repulsion at higher charge states. As the charge states increase, the molecules extend exposing protonated sites to the incoming base. The physical expansion of the molecule at higher charge states has been shown by Valentine and Clemmer using ion mobility experiments [40]. The 12+ state has the greatest Coulombic repulsion and is least selective towards the *R* enantiomer. In lower charge states, the molecule is more tightly folded which hinders the protonated sites from the incoming base and renders the molecule more selective towards one enantiomer. The reactivity of the 11+ charge state with the *S*-isomer suggests a transition between the tightly folded structure and one that is extended.

Table 2
Rate constants[a] of deprotonation reactions involving *R*- and *S*-1-amino-2-propanol and racemic mixtures with multiply charged cytochrome *c* ions produced in a 49.5/49.5/1.0 H_2O/MeOH/HOAc solution

Charge states[b]	(2*R*)-1-Amino-2-propanol	(2*S*)-1-Amino-2-propanol	*R*/*S* 50:50
10+ to 9+	67	41	37
9+ to 8+	11	4.3	4.0
8+ to 7+	6.0	3.0	2.1
9+ to 8+	46/6 (36:64)[c]	27/3 (27:73)[c]	5.6
8+ to 7+	5.0	3.0	1.8

[a] $\times 10^{-12}$ of cm^3/molecule s.
[b] The higher charge state in each group is isolated from the ion source. All others are formed by deprotonation reactions.
[c] Percent contribution from the fast and slow reacting species.

3.2. Reactions of (2R)- and (2S)-1-amino-2-proponal with 6+ to 10+ charge states

Rate constants of the more basic compounds (2*R*)- and (2*S*)-1-amino-2-propanol (estimated to be 1–2 kcal/mol more basic than 2-butylamine [41]) are presented in Tables 2 and 3. In addition to their chirality, these compounds were chosen for the possible orienting effect of the hydroxyl group. Although the higher basicity may decrease chiral specificity, the orienting effect of the hydroxyl group was thought to provide specific hydrogen bonding interactions in the adduct species that would promote greater specificity.

The results show (Table 2 and 3) again a preference for the *R* isomer. Because the compound is more basic, the preference is indeed less pronounced. The rate constant of the *R*-isomer is at most only two times greater than the *S*. Nonetheless, the system provides another example of chiral specificity in gas-phase deprotonation reactions. The selectivity for the *R*-enantiomer also decreases at high charge states. The rate constant for the deprotonation reaction of 10+ species is only 50% greater for the *R* than the *S*. For the 9+ charge state reacting with the *R*-isomer, it is nearly twice as large as with the *S*.

Cytochrome *c* ions produced from either a MeOH/H_2O mixture or an acidified MeOH/H_2O solution yield similar rates. The two methods of sample preparation again do not apparently produce very different rates. For example, the reaction of the *R* isomer with the 8+ species prepared from a 50:50 MeOH/H_2O mixture and the acidified 50:50 MeOH/H_2O mixture yield similar rate constants, (6.0×10^{-12} and 5.0×10^{-12} cm^3/molecule s, respectively). Multiple reacting species are observed only with the 9+ charge state with both *R*- and *S*-isomer. The high basicity of the reacting amine may make the reaction less selective and less sensitive to the presence of multiple populations.

Table 3
Rate constants[a] of deprotonation reactions involving *R*- and *S*-1-amino-2-propanol and racemic mixtures with multiply charged cytochrome *c* ions produced in a 50:50 MeOH/H_2OAc solution

Charge states[b]	(2*R*)-1-Amino-2-propanol	(2*S*)-1-Amino-2-propanol
8+ to 7+	6.0	2.7
7+ to 6+	<1.0	<0.6
7+ to 6+	3.5	2.0
6+ to 5+	1.8	1.0

[a] $\times 10^{-12}$ of cm^3/molecule s.
[b] The higher charge state in each group is isolated from the ion source. All others are formed by deprotonation reactions.

3.3. Reaction of racemic mixture of 1-amino-2-propanol with 8+ to 10+ charges states of cytochrome c

To further explore the nature of the chiral specificity, experiments with racemic mixtures of alkyl amines were performed. A 50:50 *R*/*S* mixture is expected to have rate constants that are averages of the pure *R* and pure *S*. Ideally, the decay of the signal for the charge state should follow a double exponential behavior. However, the rates are sufficiently similar so that deconvoluting the two exponential curves is difficult. We examined proton transfer reaction rates with racemic mixtures composed of 50% *R* and 50% *S* from a commercially obtained racemic mixture and a mixture produced by combining enantiomeric pure compounds. In both cases, the vapors of the resulting mixtures were introduced into analyzer chamber as before and allowed to react with the trapped ions. The two mixtures produce nearly iden-

tical rates. For this reason, the rate constants were averaged and are listed in Table 2. They do not have values midway between the pure *R* and the *S*. Instead, the values are generally lower than that of the *S*-isomer. In some cases, such as the 10+ and 9+ state, the rate constants of the racemic mixture equal the pure *S*-isomer, within experimental error.

Any proton transfer mechanism will involve some type of adducted species. However, the results suggest the possibility of mechanisms more complicated than that involving a singly adducted intermediate. A reaction involving this type of an intermediate has to yield rate constants that are averages of pure *R* and pure *S* when the racemic mixture is reacted. On the other hand, if instead the reaction involves a diadducted species, then intermediates are formed with three possible combinations corresponding to *RR*, *SS*, and *RS*. The three would then have different reactivities and rate constants.

3.4. Double resonance experiments to probe the presence of a diadducted species

The presence of "diadduct" intermediates cannot be easily verified. However, the role of the diadduct can be probed by double resonance experiments. These experiments entail the continuous ejection of the reaction intermediate during the entire reaction period. The effects of the ejection are monitored by observing the intensity of the reaction product. The diadducted species are not observed in appreciable abundances during the reaction; their intensities are typically less than 5%. However, their weak intensities do not preclude them from playing a key role in the proton transfer reactions. In the proton transfer of singly charged peptides, monoadducts are often not observed even in instances where proton transfer reactions occur [33–35]. Monoadducts are observed in appreciable abundances only when the gas-phase basicities of the neutral reactants are similar [34,35]. The intermediates are often short lived compared to the time scale of the detection. Fortunately, observation of the intermediate species is not a prerequisite for selective ejection.

The results of the double resonance experiments are summarized in Fig. 3. Fig. 3(a) shows the isolated 10+ charge state and the monoadduct after a reaction period of 20 s. The product ion (9+) and its corresponding monoadduct are also observed. Note that the peak corresponding to the diadduct is not readily observed (arrow). Fig. 3(b) shows the spectrum after the same reaction period with a rf burst applied to the diadduct. With an amplitude corresponding to 0.5 V

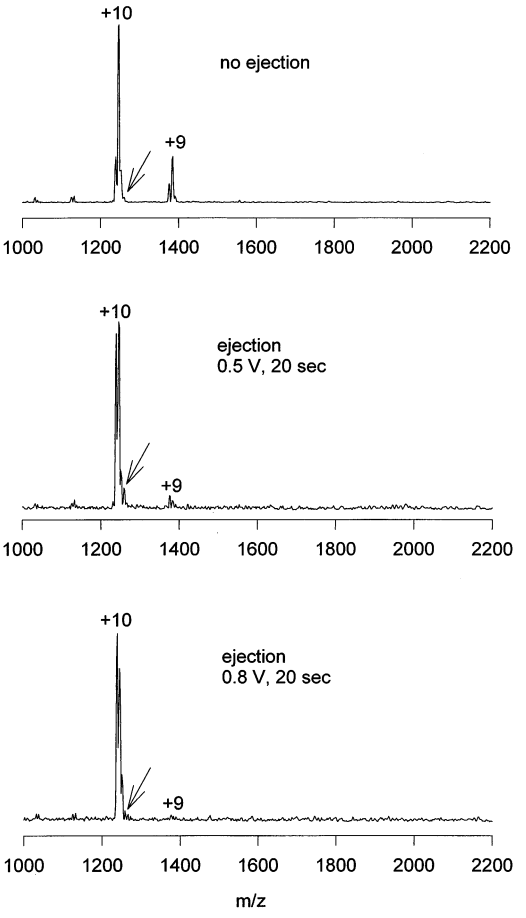

Fig. 3. Double resonance experiments involving the 10+ charge states reacting with (2*S*)-1-amino-2-propanol. (a) FTMS spectrum of the isolated 10+ charge state with the monoamine adduct and the 9+ product with its corresponding adduct. The reaction period is 20 s and the pressure of the amine is 1×10^{-7} Torr. The arrow points to the position of the diadducted complex. (b) Spectrum after a rf burst is applied to the diadducted position. The burst corresponds to 0.5 V for (base to peak) lasting the entire reaction period. (c) Spectrum with a more intense rf burst corresponding to 0.8 V (base to peak).

(base-peak), the signal corresponding to the 9+ product ion is attenuated by 20% relative to the peak in the unirradiated experiment. Increasing the amplitude of the rf burst further to 0.8 V (*b-p*) totally eliminates the intensity of 9+ charge state from the spectrum [Fig. 3(c)].

The results are promising but do not rule out at least one other possibility. Because of the relatively low resolution of the instrument, it is not possible to eject only the diadducted species. Indeed, the abundance of the monoadduct is severely attenuated during the experiment. In Fig. 3(a) the monoadduct is nearly 5 times as abundant as the 10+ species. During the ejection experiments [Figs. 3(b) and (c)], the adduct is about the same size as the uncomplexed 10+ species. The abundance of the 9+ species, adducted and non-adducted, will invariably be affected by the attenuation of the monoadduct 10+ species. It is not possible to eject the diadducted 10+ species without affecting the abundance of the 10+ monoadduct. These experiments need further refinement and access to a higher magnetic field FTMS instrument.

3.5. Temperature dependence proton transfer reactions

For chiral specificity to take place, there must be an associated barrier in the proton transfer reaction. To probe further the nature of the potential surface, temperature dependent proton transfer reactions were performed. The reactants and products were monitored and the rate constants were determined for selected charge states at the various temperatures. A typical Arrhenius plot is shown with the 8+ charge state reacting with (2*S*)-1-amino-2-propanol to produce the 7+ charge state (Fig. 4). The activation barrier is obtained from the slope in the usual manner and the pre-exponential factor from the *Y* intercept. The activation barriers and the pre-exponential factors for the reactions of the 9+, 8+, and 7+ charge states obtained from both the source and through ion/molecule reactions are listed in Table 4.

The 9+ and 8+ charge states generated from the ion source have slightly higher activation barriers than ions formed from ion/molecule reactions. The 9+ ion from the source reacts with a barrier 2.8 kcal/mol higher than the same charge state generated by the deprotonation of 10+ species. Similarly, the deprotonation of the 8+ species generated directly form the source is associated with a barrier that is 1.8 and 1.6 kcal/mol, respectively, higher than the ions produced by the deprotonation of the 9+ and 10+ states. The results suggest that ions produced by ion/molecule reactions are slightly more stable towards deprotonation reactions than ions produced directly from the ionization source.

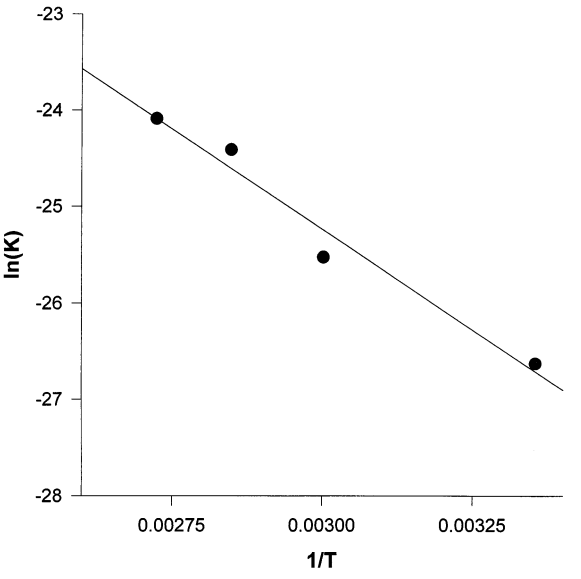

Fig. 4. The Arrhenius plot of the 8+ charge state reacting with (2*S*)-1-amino-2-propanol.

Table 4
Activation barrier (E_a) and pre-exponential factor (A) derived from the proton transfer reactions of cytochrome *c* and (2*S*)-1-amino-2-propanol

	E_a (kcal/mol)	A
Reaction of 9+ from		
9+	9.4	1×10^{19}
10+	6.6	5×10^{17}
Reaction of 8+ from		
8+	8.3	2×10^{18}
9+	6.5	9×10^{16}
10+	6.7	1×10^{17}
Reaction of 7+ from		
8+	9.7	5×10^{18}

The pre-exponential factors for the deprotonation reactions are generally large and range from 10^{16} to 10^{19}. These values are consistent more with a simple bond cleavage or dissociation reaction rather than with a series of rearrangement reactions [42,43]. The proton transfer reaction of peptides and proteins will likely involve a series of rearrangement reactions accompanied by a significantly lower *A* factor.

These results illustrate the presence of activation barriers for proton transfer reactions. However, the physical meaning of the determined values is not readily apparent. There are several complicating factors including heat induced conformational changes in the trapped protein during the experiments. Furthermore, these values suggest a stronger correspondence with the dissociation of the complex rather than a series of rearrangement reactions followed by dissociation. Even if these values are a reflection of only the dissociation barrier, they still provide important clues regarding the proton transfer reaction. The results presented here are still somewhat preliminary at best. Given the seemingly complex nature of these reactions, it seems appropriate to study their temperature dependencies in greater detail.

4. Discussion

4.1. Multiple reaction populations with the same charge states

The presence of charge states with multiple reactivities is also noted in the earlier article [29]. For ions produced from acidified and nonacidified mixtures of H_2O/CH_3OH (50:50), charge states with multiple reacting populations are observed with 2-butylamine for the 8+ and 7+, but not the 9+ state. With the 1-amino-2-propanol, only the 9+ charge state exhibits multiple populations. There are now sufficient evidence in other proton transfer reactions, H/D exchange reactions, and ion mobility studies to confirm the presence of multiple conformers with specific charge states [44–49]. The results obtained in this work are, in part, consistent with the results of cytochrome *c* ions investigated with H/D exchange by McLafferty using FTICR [46]. For the 7+ and the 8+ charge states, at least two reacting populations are observed in the chiral reaction while two and three reacting populations, respectively, are observed in the H/D exchange. For the 9+ state only one is observed with 2-butylamine, while two is observed with 1-amino-2-propanol. H/D exchange studies suggest a single population for the 9+ state. The 10+ state shows one reacting species in the chiral reaction while H/D exchange shows one dominant species and two minor species. The 11+ charge state shows two reactive species in the chiral reaction and two dominant reacting species in the H/D exchange. For the 12+ state, the H/D exchange study shows two reactive species but the chiral reactions show only one. The discrepancies are probably related to the higher sensitivity of H/D exchange towards different conformers compared to deprotonation reactions. To observe H/D exchange reactions, reagent molecules (D_2O or CH_3OD) must interact with the ion numerous times. H/D exchange reactions typically have low efficiencies [37,38,50]. Deprotonation reactions are generally faster requiring a fewer number of interactions to produce a deprotonated product.

4.2. Gas-phase protein folding reactions

The reaction of the 12+ charge state with 2-butylamine illustrates gas-phase protein folding reactions (Table 1). The 12+ species, which exhibits only slight *R*-specificity, can be rendered more selective towards the *R*-isomer by successive deprotonation. The 11+, 10+, and 9+ charge states produced from the 12+ state also exhibit the high *R*-specificity that is observed with ions produced directly from the source. This behavior is consistent with gas-phase protein folding reactions. As the high charge state is deprotonated, Coulombic repulsion decreases causing the protein to fold. Protonation sites that were previously exposed become more shielded thereby decreasing the rates of proton transfer. Gas-phase folding and unfolding reactions with FTICR have previously been reported by Williams and McLafferty [46,51]. The results presented here are consistent with the earlier ones and suggest that the conformations of gas-phase

$$[MH_n]^{n+} + B \rightleftharpoons [MBH_n]^{n+} \rightleftharpoons [MH_{n-1}]^{n-1} + BH^+$$

Scheme 2

biomolecules are indeed very fluid varying primarily with charge. Similar conclusions using ion mobility experiments have been made as experiments show systematically increasing collision cross sections accompany increasing charge states [40].

In situations where multiple conformers are observed, the less reactive species appear to be produced by the deprotonation of a higher charge state. For example, the reaction of 11+ produced by the deprotonation of 12+ with (2*S*)-2-butylamine has a rate constant that is equal to the slower reacting component of the 11+ state isolated directly from the source (4.4 and 4.3 $\times$ 10^{-12} cm^3/molecule s, respectively). Similarly, the 8+ state produced by ion-molecule reaction from the 9+ state has a rate constant that equals that of the corresponding slow reacting component of 8+ isolated from the source (2.8 and 1.6 $\times$ 10^{-12} cm^3/molecule s, respectively). These values are consistent with notion that ions produced by electrospray ionization produce metastable conformers due to the sudden (irreversible) production of ions while those produced by ion/molecule reactions are more stable conformers produced by reversible equilibrium reactions [46,52].

It should be noted that because of the long trapping times in FTICR and the presence of a deprotonating reagent, the lower charge states are probably a combination of ions that are produced from the source and through ion/molecule reactions, with the slowly reacting species coming primarily from the latter.

4.3. Mechanism of proton transfer reaction

The mechanism usually invoked for the proton transfer reactions of multiply charged proteins involve the production of an adduct intermediate $[MBH_n]^{n+}$ (Scheme 2) followed by proton transfer within the complex and dissociation to produce a net transfer of a proton. This mechanism is the same as that typically used to describe proton transfer reactions in singly charged species. The corresponding potential energy diagrams for proton transfer reactions involving multiply protonated species should be somewhat similar to the well-known double well potential with the exception of the Coulombic barrier [53,54]. The nature of this barrier is better understood by considering the reverse reaction that is best described as a singly charged amine reacting with a multiply charged reagent. The reaction encounters a barrier due to the Coulombic interaction of the singly charged species with the multiply charged one [48,55,56]. By microscopic reversibility, a similar Coulombic barrier results in the forward reaction.

Although gas-phase proton transfer reactions involving closed shell, singly charged ions are commonly thought to have no activation barriers, there are several notable exceptions. The deprotonation of Brønsted acids with polyatomic bases have long been known to have (perhaps several) transition states [57]. Steric effect can also produce an activation barrier in gas-phase processes. It has been shown earlier with substituted phenyls [58] and in this laboratory with peptides composed of bulky *R* groups such as valine [34], that steric interactions can significantly decrease the rate of proton transfer. The large sizes of the proteins and the presence of branching near the base sites of the neutral base should similarly produce a steric barrier that may account for the differences in reactivities of the enantiomers. Therefore, proton transfer reactions involving multiply protonated proteins should have at least two activation barriers due to steric and Coulombic interactions. The steric barrier is expected to be encountered earlier in the reaction coordinate than the Coulombic barrier. Steric interactions are more intimate and are governed by van der Waals radii ($1/r^3$ for dipole–dipole interactions). They occur at distances that are significantly shorter than Coulombic interactions of point charges that are governed by $1/r$ interactions.

A hypothetical potential energy diagram with two activation barriers corresponding to a steric and a Coulombic barrier is illustrated in Scheme 3. The relative height of the steric barrier may or may not be comparable to the Coulombic barrier. The reactants, a protein and a single neutral base first combine to form an ion–dipole complex. The resulting intermediate is strongly supported by experiments as the correspond-

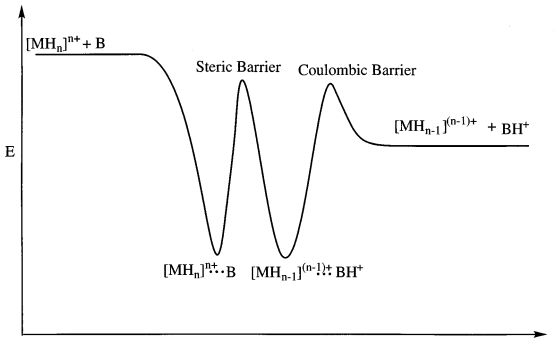

Scheme 3

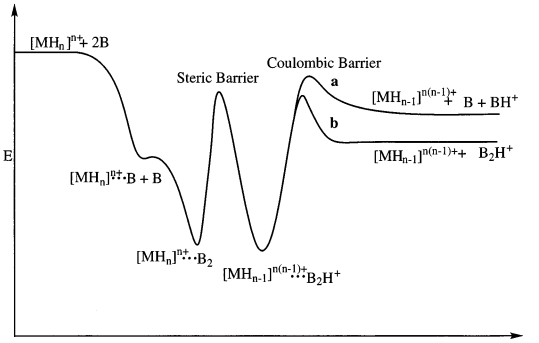

Scheme 5

ing adduct is readily observed throughout the reaction period. Its formation and the reverse dissociation are fast, as shown by the experiments, equaling the collision rates (vida infra). From this point, proton transfer occurs through a steric barrier to produce the charge transfer intermediate. Dissociation of the complex over the Coulombic barrier follows to produce the deprotonated amine.

The results of the racemic mixture and the double resonance experiment both suggest the presence of diastereomeric intermediates. These species are present only in systems where the monoadduct is already observed. If the monoadduct is not observed, then there is little probability that the diadduct is formed. A reaction sequence involving a diadducted intermediate is formulated that is analogous to the sequence involving the monoadducted intermediate (Scheme 4). In this mechanism, an additional intermediate is formed composed of a diadduct with two interacting amines to produce three different intermediates $[MB_2H_n]^{n+}$ when two chiral amines are present. The two amines (identified collectively as B_2) can be composed of *RR*, *RS*, and *SS* constituents. The mechanism now contains three intermediates with distinct reactivities. The complex can dissociate to produce a single adduct and a protonated amine (pathway a) or a proton-bound amine dimer (pathway b).

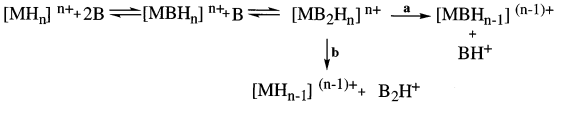

Scheme 4

An accompanying hypothetical potential energy diagram for Scheme 4 is shown in Scheme 5. The monoadduct complex forms first, as observed experimentally, followed by the addition of a second amine. Proton transfer occurs over the steric barrier to produce the protonated amine dimer. The diadducted species dissociates by one of two ways, stepwise to lose a single protonated amine or simultaneously to lose a protonated amine dimer. Pathway a is the higher energy product as the formation of the protonated amine dimer is more favorable. Experiments are underway to probe which pathway is operative. Unfortunately, this work is currently complicated by instrument limitations that prohibit the monitoring of the protonated amine or the protonated dimer.

Values for activation barriers (E_a) and the preexponential factors (A), obtained from the temperature studies, do not readily corroborate the steric barrier as the rate limiting step. The small E_a's (between 6 and 9 kcal/mol) represent reasonable reaction barriers. However, the large A factors (10^{16}–10^{17}) are more consistent with simple dissociation reactions, possibly the dissociation of the charge transfer complex. It suggests the possibility that the dissociation of the trimeric complex is the rate limiting step. The rate of this dissociation may depend on whether the two amines that are *RR*, *SS*, or *RS*.

5. Conclusions

Chiral specificity is observed in the reaction of chiral base with various charge states of cytochrome

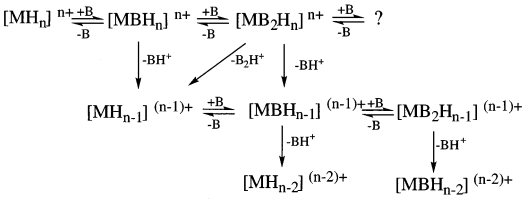

Scheme 6

c. Specific enantiomers are preferred over another by as much as tenfold. Increasing the basicity of the neutral amine decreases the specificity of the reaction.

Gas-phase proton transfer reactions involving multiply charged proteins and neutral bases (normally amines) are probably more complicated than simply the association of the neutral base and the ion followed by the dissociation of the charge transfer complex. It may even be more complicated than the two-step association mechanism depicted in Scheme 4 as there are other possible channels that can provide the observed product. A more detailed mechanism that involves other possible pathways is depicted in Scheme 6. Higher order adducts may play a role in some proton transfer reactions. Dissociation of the complex may similarly undergo various pathways and produce a variety of adducted species. The exact pathways may differ depending on the proton affinity of the base and the apparent proton affinity of the charge state. It is clear, that more detailed studies exploring all possible pathways are necessary.

Acknowledgements

Funding from the National Science Foundation is gratefully acknowledged. The authors also wish to thank Professor Robert Squires for his helpful suggestion.

References

[1] D.R. Goodlett, P.A. Abuaf, P.A. Savage, K.A. Kowalski, T.K. Mukherjee, J.W. Tolan, N. Corkum, G. Goldstein, J.B. Crowther, J. Chromat. A 707 (1995) 233.
[2] H.R. Buser, M.D. Muller, Anal. Chem. 67 (1995) 2691.
[3] M. Sawada, Y. Takai, H. Yamada, S. Hirayama, T. Kaneda, T. Tanaka, K. Kamada, T. Mizooku, S. Takeuchi, K. Ueno, K. Hirose, Y. Tobe, K. Naemura, J. Am. Chem. Soc. 117 (1995) 7726.
[4] R.L. Sheppard, X.C. Tong, J.Y. Cai, J.D. Henion, Anal. Chem. 67 (1995) 2054.
[5] A. Glausch, J. Hahn, V. Schurig, Chemosphere 30 (1995) 2079.
[6] F. Li, S.F. Cooper, M. Cote, C. Ayotte, J. Chromat. B-Biomed App. 660 (1994) 327.
[7] Y. Shinohara, K. Nagao, N. Akutsu, S. Baba, J. Pharm. Sci. 83 (1994) 1521.
[8] M.D. Muller, H.R. Buser, Anal. Chem. 66 (1994) 2155.
[9] H.J.P. Sievert, Chirality 6 (1994) 295.
[10] N.J. Haskins, M.R. Saunders, P. Camilleri, Rapid Commun. Mass Spectrom. 8 (1994) 423.
[11] D. Zimmer, V. Muschalek, J. Chromat. A 666 (1994) 241.
[12] M. Sawada, Y. Okumura, H. Yamada, Y. Takai, S. Takahashi, T. Kaneda, K. Hirose, S. Misumi, Org. Mass Spectrom. 28 (1993) 1525.
[13] H.R. Buser, M.D. Muller, Environ. Sci. Technol. 28 (1994) 119.
[14] H.R. Buser, M.D. Muller, Environ. Sci. Technol. 27 (1993) 1211.
[15] T. Sakamoto, Y. Ohtake, M. Itoh, S. Tabata, T. Kuriki, K. Uno, Biomed. Chro. 7 (1993) 99.
[16] H.R. Buser, M.D. Muller, C. Rappe, Environ. Sci. Technol. 26 (1992) 1533.
[17] M. Worner, P. Schreier, Phytoch. An. 2 (1991) 260.
[18] A. Bernreuther, P. Schreier, Phytoch. An. 2 (1991) 167.
[19] Y. Itabashi, L. Marai, A. Kuksis, Lipids 26 (1991) 951.
[20] G. Hofmeister, J.A. Leary, Org. Mass Spectrom. 26 (1991) 811.
[21] H.J. Yang, Y.Z. Chen, Org. Mass Spectrom. 27 (1992) 736.
[22] Y.P. Tu, G.Y. Yang, Y.H. Liu, S.N. Chen, Y.Z. Chen, Org. Mass Spectrom. 26 (1991) 645.
[23] Y.P. Tu, Y.Z. Chen, S.N. Chen, M.L. Wang, Z.Z. Jing, Org. Mass Spectrom. 25 (1990) 9.
[24] Applications of Mass Spectrometry to Organic Stereochemistry, J.S. Splitter and F. Turecek (Eds.), VCH, New York, 1994.
[25] M. Sawada, Mass Spectrom. Rev. 16 (1997) 73.
[26] I.H. Chu, D.V. Dearden, J.S. Bradshaw, P. Huszthy, R.M. Izatt, J. Am. Chem. Soc. 115 (1993) 4318.
[27] J.P. Honovich, G.V. Karachevtsev, E.N. Nikolaev, Rapid Commun. Mass Spectrom. 6 (1992) 429.
[28] E.N. Nikolaev, T.B. McMahon, 43rd ASMS Conference on Mass Spectrometry and Allied Topics, Atlanta, GA, 21–26 May, 1995.
[29] E. Camara, M.K. Green, S.G. Penn, C.B. Lebrilla, J. Am. Chem. Soc. 118 (1996) 8751.
[30] M. Yamashita, J.B. Fenn, J. Phys. Chem. 88 (1984) 4451.
[31] M.K. Green, E. Gard, E. Camara, S.G. Penn, C.B. Lebrilla, 43rd ASMS Conference on Mass Spectrometry and Allied Topics, Atlanta, GA, 21–26 May, 1995.
[32] E.E. Gard, M.K. Green, H. Warren, E.J.O. Camara, F. He, S.G. Penn, C.B. Lebrilla, Int. J. Mass Spectrom. Ion Processes 158 (1996) 115.

[33] J.Y. Wu, E. Gard, J. Bregar, M.K. Green, C.B. Lebrilla, J. Am. Chem. Soc. 117 (1995) 9900.
[34] J. Wu, C.B. Lebrilla, J. Am. Soc. Mass Spectrom. 6 (1995) 91.
[35] J. Wu, C.B. Lebrilla, J. Am. Chem. Soc. 115 (1993) 3270.
[36] J.E. Bartmess, R.M. Georgiadis, Vacuum 33 (1983) 149.
[37] E. Gard, D. Willard, J. Bregar, M.K. Green, C.B. Lebrilla, Org. Mass Spectrom. 28 (1993) 1632.
[38] E. Gard, M.K. Green, J. Bregar, C.B. Lebrilla, J. Am. Soc. Mass Spectrom. 5 (1994) 623.
[39] M.K. Green, E. Gard, J. Bregar, C.B. Lebrilla, J. Mass Spectrom. 30 (1995) 1103.
[40] S.J. Valentine, D.E. Clemmer, J. Am. Chem. Soc. 119 (1997) 3558.
[41] S.G. Lias, J.F. Liebman, R.D. Levin, J. Phys. Chem. Ref. Data 13 (1984) 695.
[42] P.D. Schnier, W.D. Price, R.A. Jockusch, E.R. Williams, J. Am. Chem. Soc. 118 (1996) 7178.
[43] W.D. Price, P.D. Schnier, E.R. Williams, Anal. Chem. 68 (1996) 859.
[44] C.J. Cassady, S.R. Carr, J. Mass Spectrom. 31 (1996) 247.
[45] C.J. Cassady, J. Wronka, G.H. Kruppa, F.H. Laukien, Rapid Commun. Mass Spectrom. 8 (1994) 394.
[46] T.D. Wood, R.A. Chorush, F.M. Wampler III, D.P. Little, P.B. O'Connor, F.W. McLafferty, Proc. Natl. Acad. Sci. USA 92 (1995) 2451.
[47] D. Suckau, Y. Shi, S.C. Beu, M.W. Senko, J.P. Quinn, F.M. Wampler III, F.W. McLafferty, Proc. Natl. Acad. Sci. USA 90 (1993) 790.
[48] R.A. Jockush, P.D. Schnier, W.D. Price, E.F. Strittmatter, P.A. Demirev, E.R. Williams, Anal. Chem. 69 (1997) 1119.
[49] E.R. Williams, J. Mass Spectrom. 31 (1996) 831.
[50] A.M.d.l. Pena, T.T. Ndou, J.B. Zung, K.L. Greene, D.H. Live, I.M. Warner, J. Am. Chem. Soc. 113 (1991) 1572.
[51] D.S. Gross, P.D. Schnier, S.E. Rodriguez-Cruz, C.K. Fagerquist, E.R. Williams, Proc. Natl. Acad. Sci. USA 93 (1996) 3143.
[52] J.B. Fenn, M. Mann, C.K. Meng, S.F. Wong, C.M. Whitehouse, Science 246 (1989) 64.
[53] J.M. Jasinski, J.I. Brauman, J. Am. Chem. Soc. 102 (1980) 2906.
[54] C.C. Han, J.A. Dodd, J.I. Brauman, J. Phys. Chem. 90 (1986) 471.
[55] D.S. Gross, E.R. Williams, J. Am. Chem. Soc. 117 (1995) 883.
[56] D.S. Gross, S.E. Rodriguez-Cruz, S. Bock, E.R. Williams, J. Phys. Chem. 99 (1995) 4034.
[57] E.W. Redman, T.H. Morton, J. Am. Chem. Soc. 108 (1986) 5701.
[58] H.H. Büker, H.F. Grützmacher, Int. J. Mass Spectrom. Ion Processes 109 (1991) 95.